Molecular Origin of Auxetic Behavior in Tetrahedral Framework Silicates

Andrew Alderson[1,*] and Kenneth E. Evans[2]

[1]*Centre for Materials Research and Innovation, Bolton Institute, Deane Road, Bolton BL3 5AB, United Kingdom*
[2]*Department of Engineering, University of Exeter, North Park Road, Exeter EX4 4QF, United Kingdom*

(Received 11 September 2000; published 11 November 2002)

Recent analytical models for the Poisson's ratios (ν_{ij}) of tetrahedral frameworks are applied to α-cristobalite and α-quartz for the first time. Rotation and dilation of the SiO_4 tetrahedral subunits are considered. Each mechanism leads to negative ν_{31} values, whereas negative and positive values are possible when they act concurrently. The concurrent model is in excellent agreement with experiment and explains the dichotomy between negative and positive ν_{31} values in α-cristobalite and α-quartz, respectively. The predicted strain-dependent trends confirm those from molecular modeling.

DOI: 10.1103/PhysRevLett.89.225503 PACS numbers: 62.20.Dc, 46.70.Lk, 62.90.+k, 89.90.+n

Negative Poisson's ratio materials undergo lateral expansion upon longitudinal tensile loading, as well as lateral contraction under longitudinal compression. There is increasing interest in the development of these novel materials, known as *auxetic* materials [1], due to their counterintuitive behavior and also in applications where the auxetic property itself [2,3], or enhancements in other mechanical properties due to a negative Poisson's ratio [2,4], may be exploited. Man-made and natural auxetic materials and structures exist from the molecular [3,5] to the micro- [4,6] and macroscopic levels [2,7]. The discovery of auxetic behavior at the molecular level in single-crystal α-cristobalite [5] has led to more research into the modeling, design, and development of molecular auxetics [8–14]. We have recently developed analytical models in which the deformation of a tetrahedral framework structure, analogous to the molecular framework of α-cristobalite, is by tetrahedral rotation and dilation [15]. Here we use these models to examine the related α-quartz structure, and show how they explain the dichotomy between auxetic and nonauxetic behavior in these two materials.

The basic molecular "building block" for both α-cristobalite and α-quartz is the SiO_4 tetrahedron consisting of an O atom at each of the four corners surrounding a central Si atom. Both structures consist of a framework of corner-sharing SiO_4 tetrahedra in which each O atom is shared between two adjacent tetrahedra. α-cristobalite contains four tetrahedra per tetragonal primitive unit cell (space group $P4_12_12$) and α-quartz contains three tetrahedra per trigonal primitive unit cell (space group $P3_121$); see Figs. 1(a) and 1(b).

The Poisson's ratio ν_{ij} of a material under stress in the x_i direction is defined by

$$\nu_{ij} = -\frac{\varepsilon_j}{\varepsilon_i} = -\frac{s_{ji}}{s_{ii}}, \qquad (1)$$

where ε_i and ε_j are the true strains in the orthogonal x_i and x_j directions, respectively ($i, j = 1, 2,$ or 3 and $i \neq j$), and the s's are elastic compliance coefficients. Tensile strains are positive and contractile strains are negative. Hence a material which undergoes lateral expansion due to longitudinal extension has a negative Poisson's ratio. Employing the experimental elastic compliance coefficients in Eq. (1) for α-cristobalite [5] and α-quartz [16] reveals that auxetic behavior is observed in α-cristobalite but not α-quartz when loaded in the x_3 direction (Table I). Cooperative rotation of the SiO_4 tetrahedra has been suggested as the mechanism leading to auxetic behavior in α-cristobalite [5,8,9].

Assuming regular tetrahedra, the Poisson's ratios for both structures can be derived in terms of a tetrahedral tilt angle (δ) and the tetrahedral edge length (l) [Figs. 1(a) and 1(c)]. The mutually orthogonal principal axes x_1, x_2,

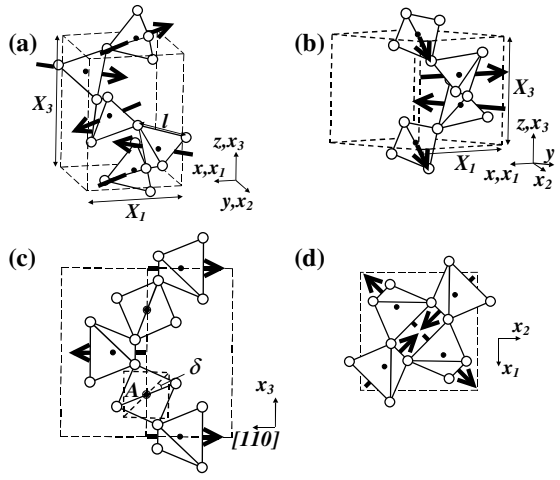

FIG. 1. Tetrahedral framework unit cells for α-cristobalite and α-quartz showing tetrahedral rotation axes (solid arrows) and geometrical parameters. Filled circles are silicon atoms; empty circles are oxygen atoms. (a) α-cristobalite–unit-cell lengths are given by $X_1 = l(1 + \cos\delta)$ and $X_3 = 2\sqrt{2}l\cos\delta$. (b) α-quartz–unit-cell lengths are given by $X_1 = \frac{l(1+\sqrt{3}\cos\delta)}{\sqrt{2}}$ and $X_3 = \frac{3l\cos\delta}{\sqrt{2}}$. (c) x_3-[110] projection of α-cristobalite, showing an "untilted" tetrahedron (A) to define the tilt angle δ. (d) x_1-x_2 projection of α-cristobalite.

TABLE I. ν_{31} Poisson's ratios for α-quartz and α-cristobalite. Expt = experimental [5,16]; CM(ai) = computer modeling *ab initio* calculations [8,9]; CM(pp) = computer modeling pair-potential calculations (method of long waves) [9]; CM(rigid) = computer modeling pair-potential calculations (rigid SiO_4 tetrahedra constraint) [8,9].

	α-quartz	α-cristobalite
Expt	$+0.127 \pm 0.001$	-0.07 ± 0.01
RTM	-0.62	-0.48
DTM	-1.00	-1.00
CTM	$+0.11$	-0.06
CM (ai)	$+0.1$	-0.2
CM (pp)	$+0.19$	-0.05
CM (rigid)	-0.6	-0.5

and x_3 and the crystallographic symmetry axes x, y, and z are also shown in Figs. 1(a) and 1(b) for both polymorphs. δ is defined with respect to an axis passing through the midpoints of two opposing edges of each tetrahedron. For α-cristobalite the tilt axes are aligned parallel to the unit-cell diagonals in the x-y plane [Figs. 1(a), 1(c), and 1(d)]; whereas they are parallel to either of the x or y axes or parallel to the short unit-cell diagonal in the$x$-y plane for α quartz [Fig. 1(b)]. $\delta = 0$ when the top edge of each tetrahedron is perpendicular to the z axis [Fig. 1(c)]. Tetrahedral rotation corresponds to a variation in δ [Fig. 2(a)], whereas l varies in tetrahedral dilation [Fig. 2(b)].

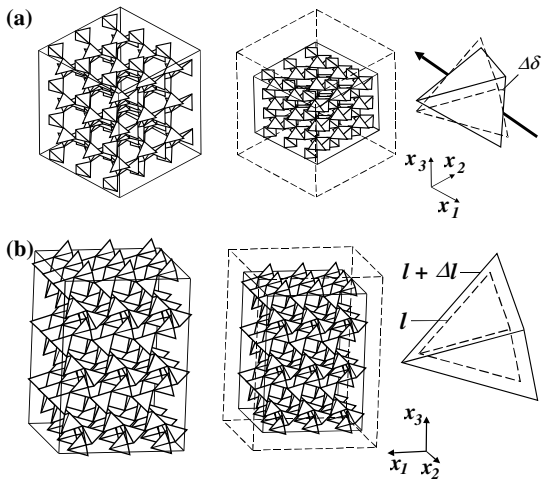

FIG. 2. Auxetic deformation mechanisms in tetrahedral frameworks. (a) Tetrahedral rotation about the tilt axis through the centers of two opposing tetrahedron edges. Fully expanded (i.e., $\delta = 0°$) and fully densified (i.e., $\delta = 45°$) $3 \times 3 \times 3$ extended tetrahedral networks are shown for the α-cristobalite structure. (b) Tetrahedral dilation in which tetrahedral size varies. $3 \times 3 \times 3$ extended tetrahedral networks for the α-cristobalite structure are shown before and after contraction of the tetrahedra (δ = same value in both cases).

Analytical expressions for the elastic constants of network structures deforming by multiple deformation mechanisms acting simultaneously have been developed for honeycombs [10] and microporous polymers [17]. Using an analogous approach, the Poisson's ratios for α-cristobalite deforming by tetrahedral rotation and dilation acting concurrently, which we call the concurrent tetrahedra model (CTM), can be readily shown [15] to take the form

$$\nu_{31} = \nu_{13}^{-1} = -\left(\frac{\cos\delta}{1+\cos\delta}\right)\left(\frac{1+\cos\delta-\kappa\sin\delta}{\cos\delta-\kappa\sin\delta}\right), \quad (2)$$

where κ is a "strength" parameter defined by

$$\kappa = l\frac{d\delta}{dl} = l\frac{d\delta}{d\theta}\frac{d\theta}{d\sec\theta}\frac{d\sec\theta}{dR}\frac{dR}{dl}. \quad (3)$$

For silica, l = O-O bond length, R = Si-O bond length, and θ = Si-O-Si angle.

Similarly, it can be shown [18] that the equivalent expression for α-quartz is

$$\nu_{31} = \nu_{13}^{-1} = -\left(\frac{\sqrt{3}\cos\delta}{1+\sqrt{3}\cos\delta}\right)\frac{\left(\frac{1}{\sqrt{3}}+\cos\delta-\kappa\sin\delta\right)}{(\cos\delta-\kappa\sin\delta)}. \quad (4)$$

Equations (2) and (4) indicate that if ν_{31} is small, then ν_{13} will be large (e.g., $\nu_{13} = 10$ if $\nu_{31} = 0.1$). A Poisson's ratio with such a large magnitude is outside of the bounds allowed by classical elasticity theory for isotropic materials ($-1 \le \nu \le +0.5$). However, for anisotropic materials it has been shown [19] that $\nu_{ij} \le (E_i/E_j)^{1/2}$ and $\nu_{ij}\nu_{ki}\nu_{jk} < 1/2$, where E_i and E_j are the Young's moduli along x_i and x_j, respectively, $k = 1$, 2, or 3 and $k \ne i \ne j$. Hence, very large Poisson's ratios are allowed for anisotropic materials. Very large negative and positive Poisson's ratios are predicted in periodic cellular solid microstructures [10,17] and "giant" Poisson's ratios have also been predicted in vacuumlike colloidal crystals [20]. Very large negative Poisson's ratios (of the order of -12) have been observed experimentally in highly anisotropic microporous polymers [6]. Hence, while they may be unusual, large Poisson's ratios are not unphysical in anisotropic materials such as the tetrahedral framework geometries considered here.

The expressions for the rotating tetrahedra model (RTM), in which deformation is assumed to be due to the cooperative rotation of rigid tetrahedra ($dl = 0$), are derived by substituting $\kappa = \infty$ in Eqs. (2) and (4). Similarly, substituting $\kappa = 0$ into Eqs. (2) and (4) yields the expressions for the dilating tetrahedra model (DTM) in which tetrahedral size variation for constant shape occurs at fixed tetrahedral orientation ($d\delta = 0$).

For both structures increasing δ leads to a decrease in the unit-cell lengths [Fig. 2(a)], whereas increasing l leads to an increase in the unit-cell lengths [Fig. 2(b)].

Hence both mechanisms act to expand (or contract) the structure for negative values of κ ($d\delta$ and dl of opposite sign). Positive values of κ ($d\delta$ and dl of equal sign) correspond to one of the mechanisms expanding the structure whereas the other contracts the structure. In this case an overall positive Poisson's ratio is possible [15].

In considering the values of κ to be employed in the CTM for the α-cristobalite and α-quartz polymorphs of crystalline silica it is instructive to use the expanded form of κ given in Eq. (3). $dR/dl\,[=\sqrt{3}/(2\sqrt{2})]$, $d\theta/d\sec\theta\,(=\cos^2\theta/\sin\theta)$, and $d\delta/d\theta$ are purely geometrical. Both polymorphs contain tetrahedra of similar size ($l \sim 2.63$ Å) and have similar intertetrahedral angles and distances ($\theta \sim 144.4$ and $146.4°$ for α-quartz [21] and α-cristobalite [22], respectively; Si...Si ~ 3.06 Å [23,24]). Hence, to a first approximation we expect the inter- and intratetrahedral forces to yield similar values of $d\sec\theta/dR$ (the amount of intertetrahedral angle change relative to tetrahedral size change) and, therefore, similar $l(d\sec\theta/dR)(dR/dl)$ values for both polymorphs if the CTM is valid. Expressions relating δ to θ have been derived elsewhere for α-quartz [25] and α-cristobalite [26]. From these expressions, it can be shown for the α-quartz structure that

$$\frac{d\delta}{d\theta}\frac{d\theta}{d\sec\theta} = -\frac{\{\frac{3}{4} - [\cos\delta + (2\sqrt{3})^{-1}]^2\}^2}{2[\cos\delta + (2\sqrt{3})^{-1}]\sin\delta}, \qquad (5)$$

and for the α-cristobalite structure that

$$\frac{d\delta}{d\theta}\frac{d\theta}{d\sec\theta} = -\frac{(1 - 2\cos\delta - 2\cos^2\delta)^2}{6[1 + 2\cos\delta]\sin\delta}. \qquad (6)$$

Hence from Eqs. (3), (5), and (6), and the above assumption that $l(d\sec\theta/dR)(dR/dl)$ is similar for both polymorphs, the ratio of the strength parameters for α-quartz and α-cristobalite are dependent only on the respective values of δ:

$$\frac{\kappa_q}{\kappa_c} = \frac{\{\frac{3}{4} - [\cos\delta_q + (2\sqrt{3})^{-1}]^2\}^2}{[\cos\delta_q + (2\sqrt{3})^{-1}]\sin\delta_q} \times \frac{3(1 + 2\cos\delta_c)\sin\delta_c}{(1 - 2\cos\delta_c - 2\cos^2\delta_c)^2}, \qquad (7)$$

where the subscripts q and c refer to α-quartz and α-cristobalite, respectively. Equation (7) yields $\kappa_q/\kappa_c = 0.9995$ when the experimental tilt angles for α-quartz [25] and α-cristobalite [23] of $\delta_q = 16.3°$ and $\delta_c = 23.5°$, respectively, are employed. Hence we expect, from simple geometrical considerations, the CTM strength parameters for α-quartz and α-cristobalite to be equal in magnitude and sign if the model is valid.

Molecular orbital calculations for α-quartz imply l increases as θ decreases (δ increases) [25] and there is experimental evidence for such a relationship between the mean Si-O length ($\propto l$) and θ in both polymorphs (e.g., Ref. [23]). This, then, corresponds to a positive value of κ in the CTM.

Substituting the experimental values of ν_{31} (Refs. [5,16]) and δ (Refs. [23,25]) into Eqs. (2) and (4) yields $\kappa = +5.24 \pm 0.10$ and $\kappa = +5.13 \pm 0.10$ for α-cristobalite and α-quartz, respectively. The two values of κ thus obtained for α-quartz and α-cristobalite are, therefore, equal in magnitude (within error) and positive, as proposed above if the CTM is valid for these materials.

The ν_{31} values calculated from all three analytical models for α-cristobalite and α-quartz are compared with experimental and computer modeling data in Table I. The analytical model calculations employed the experimental values of $\delta = 16.3°$ and $23.5°$ for α-quartz and α-cristobalite, respectively. The CTM values for both polymorphs were calculated using the average value of $\kappa = +5.18$ from the fit to the experimental data.

The RTM ν_{31} calculations are in excellent agreement with computer modeling predictions, based on classical interatomic potentials, in which the SiO_4 tetrahedra were constrained to remain rigid during deformation of both structures. Hence the role of rigid tetrahedral rotation as an auxetic deformation mechanism in tetrahedral framework silicates is confirmed. However, comparison of the experimental ν_{31} data with the RTM calculations yields poor agreement and so tetrahedral rotation alone cannot explain the deformation of these polymorphs when loaded along x_3.

The DTM calculations show that an alternative mechanism for auxetic behavior exists for these structures, although poor agreement is achieved with the experimental and computer modeling data.

For both polymorphs the CTM ν_{31} values are in excellent agreement with experiment and represent an improvement on computer modeling calculations based on classical interatomic potentials and on fully quantum-mechanical *ab initio* pseudopotentials [8,9]. Single-crystal α-quartz and α-cristobalite are, therefore, examples of two molecular materials for which the model of concurrent tetrahedral rotation and dilation is valid for loading in the x_3 direction.

The variation of ν_{31} with loading strain is shown in Fig. 3 for both polymorphs. These calculations use the expanded form of $d\delta/dl$ given in Eq. (3) to relate the change in tetrahedron edge length to the change in tilt angle at any value of δ, and assume $d\sec\theta/dR$ remains constant during deformation (which is reasonable from previous structural investigations [24,25]) at the value ($= -3.445$ Å^{-1}) corresponding to $\kappa = +5.18$ in the undeformed state. The CTM predicts ν_{31} will become positive under uniaxial compression and increasingly negative under tensile loading for α-cristobalite. For α-quartz ν_{31} is predicted to become increasingly positive under compression but is also predicted to be negative under sufficient tensile loading. These trends are in agreement with computer modeling calculations [8,9]. ν_{31} has

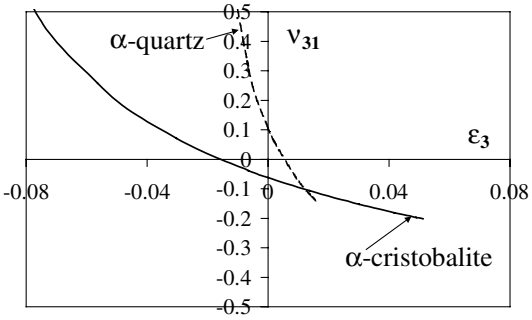

FIG. 3. ν_{31} versus loading strain ε_3 for α-quartz (dashed curve) and α-cristobalite (solid curve) calculated from the CTM. ε_3 was calculated from $\varepsilon_3 = \ln[X_3/X_{3(0)}]$ where X_3 and $X_{3(0)}$ are the deformed and undeformed unit-cell lengths along x_3 obtained by substituting the deformed and initial values, respectively, of l and δ in the expressions for α-quartz and α-cristobalite given in the caption to Fig. 1. l and δ were calculated using Eq. (3) and the assumptions outlined in the text.

also been predicted from pair-potential calculations to be negative for α-quartz under reduced hydrostatic pressure and is known to be negative at elevated temperatures (800–850 K) [27].

In conclusion, we have shown that both concurrent tetrahedral rotation and dilation are needed to explain both the positive and negative Poisson's ratios observed in α-quartz and α-cristobalite, respectively, when loaded in the x_3 direction. α-cristobalite exhibits auxetic functionality as a result of two independent auxetic mechanisms acting concurrently. α-quartz, on the other hand, provides clear evidence that two auxetic deformation mechanisms can lead to nonauxetic behavior when one (RTM) acts to expand the structure and the other (DTM) acts to contract it. The remarkable accuracy with which the values of the real materials are predicted by a model having only a few degrees of freedom indicates that tetrahedral distortion is not a significant deformation mechanism for loading along the x_3 direction. This may be attributable to the orientation of the tetrahedra with respect to this specific loading direction in these two polymorphs. On the other hand, tetrahedral distortion is known to occur in these polymorphs when subjected to thermal or hydrostatic pressure loading, and it can be shown [18] that the CTM is not a valid model for deformation under these loading conditions.

The strain-dependent variations in ν_{31} are also consistent with the trends predicted from computer modeling calculations. Having clearly identified the origin for auxetic behavior in tetrahedral framework structures we are now applying and extending the models to the germania analogs [18], and also using the general methodology and alternative modeling techniques in the drive to design and discover other molecular auxetic materials [12].

The authors acknowledge the financial support of BNFL during this work.

*To whom all correspondence and requests for materials should be addressed.
Email address: A.Alderson@bolton.ac.uk

[1] K. E. Evans, M. A. Nkansah, I. J. Hutchinson, and S. C. Rogers, Nature (London) **353**, 124 (1991).
[2] R. Lakes, Science **235**, 1038 (1987).
[3] R. H. Baughman, J. M. Shacklette, A. A. Zakhidov, and S. Stafstrom, Nature (London) **392**, 362 (1998).
[4] K. L. Alderson, A. P. Pickles, P. J. Neale, and K. E. Evans, Acta Metall. Mater. **42**, 2261 (1994).
[5] A. Yeganeh-Haeri, D. J. Weidner, and J. B. Parise, Science **257**, 650 (1992).
[6] B. D. Caddock and K. E. Evans, J. Phys. D **22**, 1877 (1989).
[7] G. Wei and S. F. Edwards, Phys. Rev. E **58**, 6173 (1998).
[8] N. R. Keskar and J. R. Chelikowsky, Nature (London) **358**, 222 (1992).
[9] N. R. Keskar and J. R. Chelikowsky, Phys. Rev. B **48**, 16 227 (1993).
[10] K. E. Evans, A. Alderson, and F. R. Christian, J. Chem. Soc. Faraday Trans. **91**, 2671 (1995).
[11] C. He, P. Liu, and A. C. Griffin, Macromolecules **31**, 3145 (1998).
[12] J. N. Grima, R. Jackson, A. Alderson, and K. E. Evans, Adv. Mater. **12**, 1912 (2000).
[13] H. Kimizuka, H. Kaburaki, and Y. Kogure, Phys. Rev. Lett. **84**, 5548 (2000).
[14] M. Bowick, A. Cacciuto, G. Thorleifsson, and A. Travesset, Phys. Rev. Lett. **87**, 148103 (2001).
[15] A. Alderson and K. E. Evans, Phys. Chem. Miner. **28**, 711 (2001).
[16] H. J. McSkimin, P. Andreatch, Jr., and R. N. Thurston, J. Appl. Phys. **36**, 1624 (1965).
[17] A. Alderson and K. E. Evans, J. Mater. Sci. **32**, 2797 (1997).
[18] A. Alderson and K. E. Evans (to be published).
[19] B. M. Lempriere, AIAA J. **6**, 2226 (1968).
[20] R. H. Baughman *et al.*, Science **288**, 2018 (2000).
[21] J. D. Jorgensen, J. Appl. Phys. **49**, 5473 (1978).
[22] W. W. Schmahl, I. P. Swainson, M. T. Dove, and A. Graeme-Barber, Z. Kristallogr. **201**, 125 (1992).
[23] J. J. Pluth, J. V. Smith, and J. Faber, Jr., J. Appl. Phys. **57**, 1045 (1985).
[24] J. Glinnemann *et al.*, Z. Kristallogr. **198**, 177 (1992).
[25] H. Grimm and B. Dorner, J. Phys. Chem. Solids **36**, 407 (1975).
[26] M. O'Keeffe and B. G. Hyde, Acta Crystallogr. B **32**, 2923 (1976).
[27] M. B. Smirnov and A. P. Mirgorodsky, Phys. Rev. Lett. **78**, 2413 (1997).